

## Cold-formed steel centre-sheathed (mid-ply) shear walls

Vincent Brière, Veronica Santos, Colin A. Rogers\*

Department of Civil Engineering and Applied Mechanics, McGill University, Montreal, QC, Canada



### ARTICLE INFO

#### Keywords:

Cold-formed steel  
Shear wall  
High-strength  
Seismic  
Structural design

### ABSTRACT

An innovative configuration for cold-formed steel (CFS) framed and sheathed shear walls developed to address the need for a ductile lateral framing system of high shear resistance appropriate for mid-rise buildings is presented in this paper. This shear wall configuration comprises a sheathing placed at the mid-line of the framing, and hence is known as either a centre-sheathed or mid-ply wall. A laboratory based research program was conducted following an iterative design, analysis and testing process. The testing included fifteen 1218 mm × 2438 mm shear walls subjected to in-plane displacement-based monotonic and cyclic loading. The test specimens were able to reach shear resistances substantially exceeding the capacity of the CFS walls listed in the AISI S400 Standard, while attaining storey drift values superior to 6% in the best case. A preliminary equation-based nominal shear strength prediction method has been developed, reflecting the shear wall's innovative configuration and superior behaviour.

### 1. Introduction

In North America the seismic design of cold-formed steel (CFS) framing systems is carried out using the American Iron and Steel Institute (AISI) S400 Standard [1]. This document contains design requirements for the following light frame vertical systems; shear walls with wood-based structural panels, shear walls with steel sheet sheathing, shear walls with gypsum board or fiberboard panels, strap braced walls and special bolted moment frames. This design information focuses on residential and low-rise building construction; it is limited with respect to the higher capacity lateral systems required for use in mid-rise construction. However, the CFS industry's desire to construct buildings in the mid-rise range has demonstrated a need for lateral systems of improved shear strength and resiliency.

The objective of the research described in this paper was to develop a cold-formed steel framed and steel sheathed shear wall system with more than double the capacity of the walls currently listed in AISI S400 and having the ability to carry these loads at drift levels that surpass the range observed in past CFS wall tests (approx. 2–3%). This was achieved by developing a new configuration of shear wall known as either the centre-sheathed or mid-ply wall. The scope of study included a series of tests in which this wall configuration was initially evaluated and then improved through design iterations. Furthermore, a preliminary design method has been created to aid in the prediction of nominal shear wall resistance and member selection. A description of the test program and preliminary design method is provided herein.

#### 1.1. Background of steel sheathed cold-formed steel framed shear wall systems

The design provisions found in the AISI S400 Standard [1], the "North American Standard for Seismic Design of Cold-formed Steel Structural Systems", have been developed over the past decades through various research programs. Specific to shear walls sheathed with thin steel panels, design values for the USA and Mexico were obtained from research carried out by Serrette et al. [2,3], which was followed by studies by Yu et al. [4], Yu and Chen [5,6], Yu [7] and Ellis [8]. This work was complemented by additional studies undertaken to develop a seismic design approach for use in Canada. This included dynamic shake table testing of single and double-storey shear walls by Shamim et al. [9], as well as numerical modelling of representative CFS buildings subjected to ground motions by Shamim and Rogers [10,11]. Further testing on various size walls sheathed with steel panels on a single side, and walls with additional frame blocking was completed by DaBreo et al. [12], which was followed by an article by Balh et al. [13] describing the design approach now found in the AISI S400 Standard [1].

Other recent studies, on steel sheathed shear walls constructed of a CFS frame have also been carried out; for example Xie et al. [14] investigated the performance of steel sheathed shear walls in which the sheathing was attached with rivets instead of screws. Attari et al. [15] and Javaheri-Tafti [16], among others, have further studied the performance of walls with flat steel sheathing. Researchers have also

\* Correspondence to: 817 Sherbrooke Street West, Montreal, QC, Canada H3A 0C3.

E-mail addresses: [vincent.briere@mail.mcgill.ca](mailto:vincent.briere@mail.mcgill.ca) (V. Brière), [veronica.santos@mail.mcgill.ca](mailto:veronica.santos@mail.mcgill.ca) (V. Santos), [colin.rogers@mcgill.ca](mailto:colin.rogers@mcgill.ca) (C.A. Rogers).

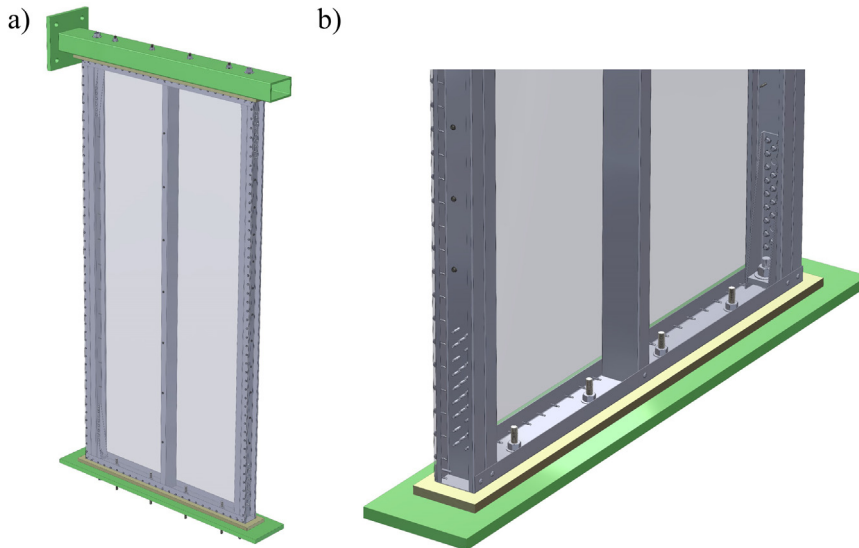


**Fig. 1.** Typical single-sheathed CFS shear wall configuration as per AISI S400 [1]; a) overall view, b) detailed view of base.

investigated the use of corrugated steel panels on shear walls in place of flat sheets [17–19]. A detailed review paper by Sharafi et al. [20] provides a broader summary of the various research projects on lateral force resisting systems composed of cold-formed steel frames.

The steel sheathed shear wall configuration for which tabulated shear resistance values are provided in the AISI S400 Standard is that of a CFS framed wall sheathed on a single side with thin steel panels (Fig. 1). Attempts to improve the resistance of such walls were made by DaBreo et al. [12], in which full frame blocking was installed between stud members to restrict the torsional deformations of the chord studs. Due to the eccentric placement of the sheathing, the chord studs of the wall are subjected to torsional moments, which can lead to their failure during ground motion excitation. This blocking technique proved to function well; as such, a specific shear wall configuration of this construction with nominal shear resistance values approaching 30 kN/m was added to the AISI S400 Standard. To further expand on this reinforcement technique, Rizk [21] completed a series of blocked wall tests, of shorter and longer lengths than DaBreo et al., to ascertain whether these different aspect ratio walls would also benefit from this form of stud bracing. Rizk showed that even with the frame blocking, as the sheathing thickness was increased and/or the number of sheathing fasteners was increased the chord studs could become damaged due to unwrapping of the cross-section (Fig. 2a). Furthermore, he observed that for long walls, i.e. 2440 mm in length, the frame blocking was not sufficiently rigid to fully restrict the torsional deformation of the wall as a whole. The interior studs of the wall were deformed out-of-plane due to the eccentric placement of the sheathing panels, which has led to an out-of-plane loading on the structural members of the wall (Fig. 2b). Given these findings, and the desire to construct steel sheathed CFS walls with greater shear resistance, Brière [22] and Santos [23] then carried out tests of double-sheathed walls, a configuration that is permitted by AISI S400, in which the chord members were made of built-up box shapes to further improve their torsional strength and stiffness. A substantial increase in resistance was measured, to levels approximately twice that found for the single-sheathed walls listed in the AISI S400 Standard. However, the ductility of these walls, as measured through a comparison of the yield displacement (drift) versus the in-plane displacement at the 0.8 post-peak strength level, did not show improvement over that measured for the standard configuration of shear wall by Rizk [21], DaBreo et al. [12] and Yu [7], among others. As shown in Fig. 2c, which contains a photo of a double-sheathed wall tested by Brière [22] and Santos [23], the reversed-cyclic nature of the in-plane loading, which causes bearing related slotting of the steel

sheathing, in combination with the shear buckling deformations of the steel sheathing, led to the panels pulling over the heads of the screws and a loss in the shear resistance. This same behaviour was observed in the conventional walls tested by Rizk [21], DaBreo et al. [12] and Yu [7]. In light of the findings of the various research programs summarized in this section, it was proposed to develop a wall in which both the torsional loading aspect and restricted ductility of the standard configuration CFS shear wall could be overcome. In this endeavour, the centre-sheathed (mid-ply) CFS shear wall was conceived. The following sections in this article describe the process by which this new shear wall configuration was developed and the resulting performance under in-plane lateral loading.

## 2. Design and experimental program of centre-sheathed (mid-ply) shear wall configuration

Cold-formed steel sheathed and framed shear walls resist in-plane lateral loads via a combination of tension and compression forces developed in the sheathing panels. Given the typical thin steel sheathing used in the construction of these walls, the applied shear forces result in the shear buckling of the panel, while an associated tension force develops over a restricted width ( $W_e$ ), often referred to as the tension field (Fig. 3a). The level of resistance reached by the wall will vary depending on the parameters used for its construction, e.g. screw spacing, screw size, panel thicknesses, and steel grade, assuming that the framing members are protected from failure by using a capacity-based design approach. A conventionally constructed CFS shear wall for which the sheathing is undergoing shear buckling and also carrying a tension field is shown in Fig. 3b. In the design of an improved variant of CFS shear wall, the prediction of the tension field effects is necessary.

### 2.1. Development of a new shear wall configuration

The experimental programs carried out by Rizk [21], DaBreo [12] and others using a CFS framed shear wall with a thin steel panel screw-connected to a single face of the wall showed an overall good resistance and ductility. However, the loading eccentricity caused by the placement of the sheathing was limiting, in that it may result in failure of the chord studs, which are subjected to increasing torsion as the panel thickness and number of screws is raised. Furthermore, the sheathing imposed out-of-plane forces, caused by its shear buckling, on one face of the wall, which loaded the centre studs out-of-plane and reduced their ability to carry gravity loads. Frame damage must be avoided due

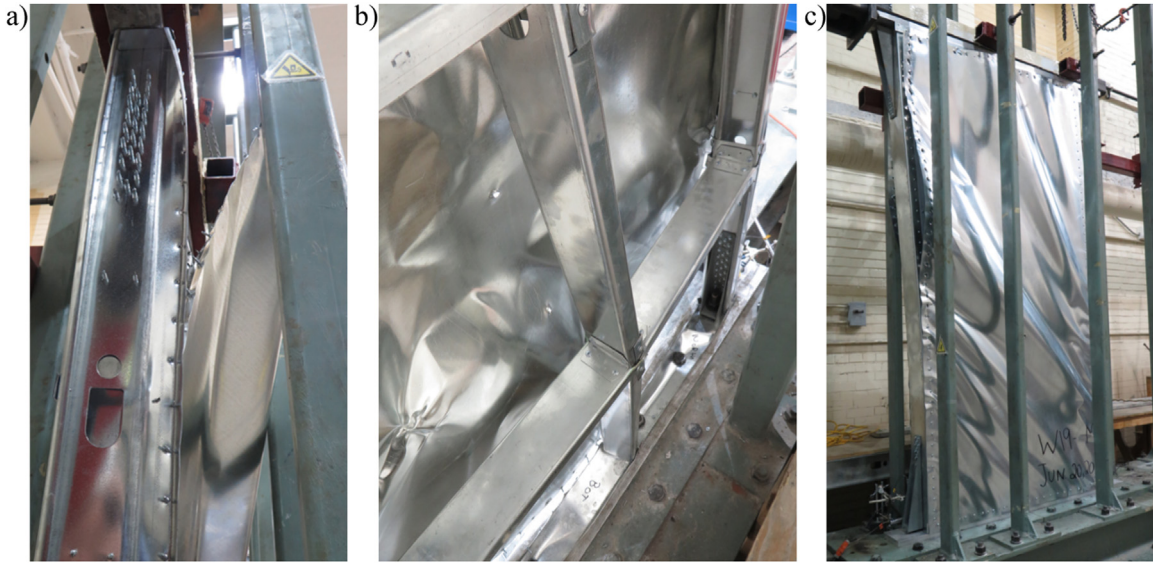


**Fig. 2.** Damage to steel sheathed shear walls as observed by Rizk [21], Brière [22] and Santos [23] due to: a) torsional forces on chord studs, b) out-of-plane forces on blocked centre stud, and c) loss of connection to steel panel in double-sheathed wall configuration.

to the need for post-earthquake resistance to gravity loads and to maintain shear resistance during a seismic event. Therefore, minimizing the eccentric loading caused by the sheathing being placed on one side of a wall became the first main objective for the new shear wall configuration such that shear resistance values exceeding those listed in AISI S400 could be achieved.

This led to the design of walls by Brière [22] and Santos [23] using sheathing placed on both sides, i.e. the double-sheathed configuration. Built-up box chord studs were used to accommodate the higher lateral forces. The symmetric placement of the two sheathing panels allowed for the torsional loading on the chord studs to be minimized, and hence the shear resistance of the wall was significantly improved. However, the ductility of the walls was not enhanced due to the sheathing pulling over the heads of the screw fasteners.

To achieve a stronger and more ductile CFS shear wall the innovative centre-sheathed (mid-ply) configuration (Fig. 4) was then

conceived. In this configuration the 1218 mm × 2438 mm walls were detailed to centrally confine the sheathing within the framing, which provided for a substantial increase in both shear resistance and ductility in comparison with the walls having external sheathing on one or both sides. The steel panel was sandwiched by built-up vertical studs along the edges and horizontal members located at the base and top of the wall. The concept was to have symmetric loading on the framing members, to remove torsional forces on the chord studs and to confine the sheathing such that it could not disengage from the screws. The central stud was excluded from this configuration since the out-of-plane forces due to shear buckling of the sheathing would damage it. Consequently, the top horizontal member is required to act as a beam transferring any point loads originating from the upper floor or roof framing members into the chord studs. The connection between the vertical and horizontal framing members had to be adjusted accordingly. Because this configuration precluded the eccentric loading within

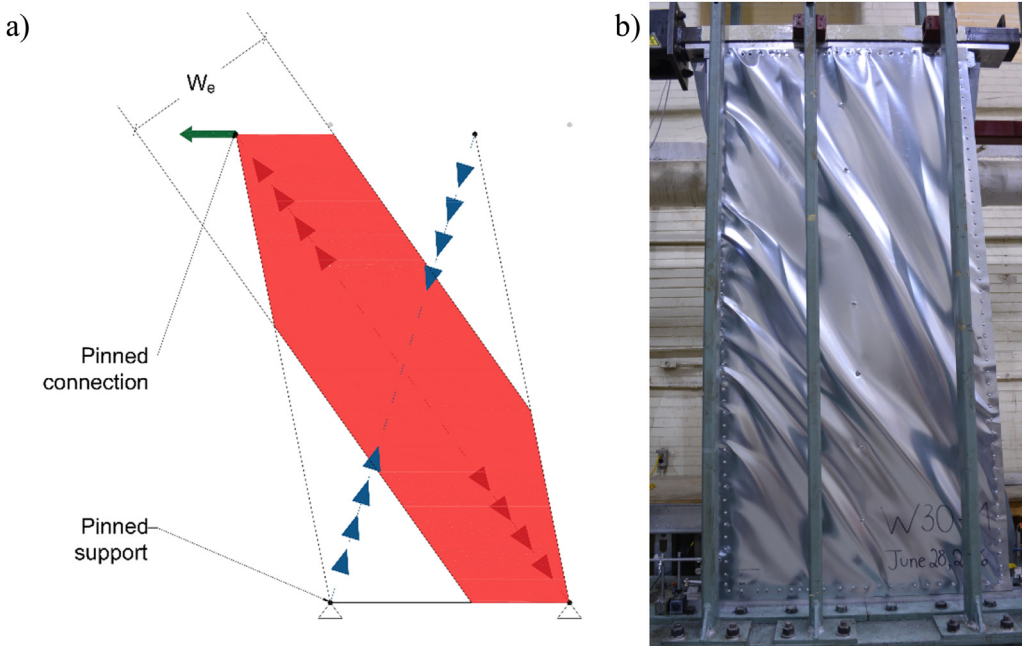


**Fig. 3.** Shear wall behaviour; a) Tension field representation, and b) shear buckling and tension field in a single-sided steel sheathed shear wall configuration.

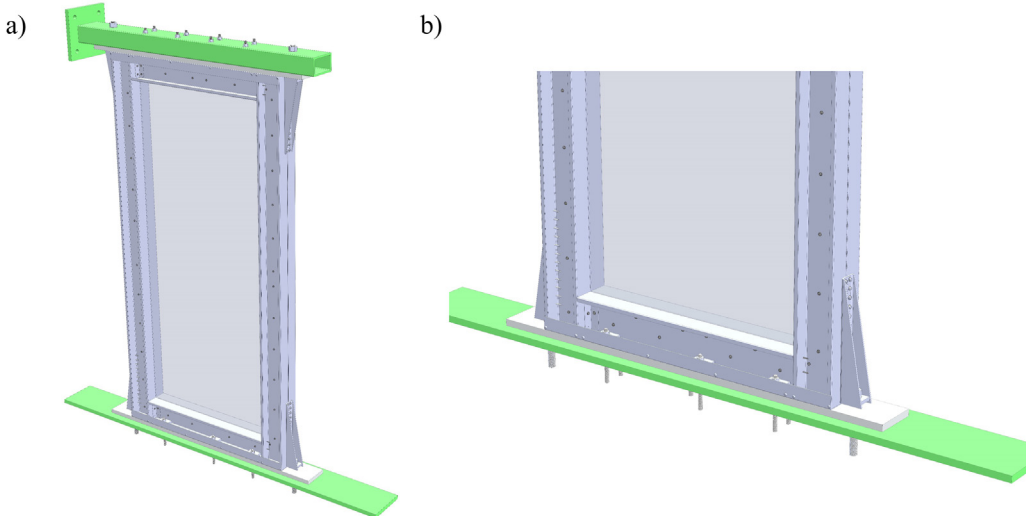


**Fig. 4.** Initial centre-sheathed configuration W18-M installed in test frame; a) overall view, b) detailed view of base (sheathing shown as transparent).

the shear wall, it allowed for the removal of the requirement for the frame blocking as used in the testing by DaBreo et al. [12] and Rizk [21]. In addition, it gave the opportunity to increase the thickness of the sheathing and number of fasteners, with the objective of reaching higher shear resistance, since the torsional forces responsible for damage in the chord studs and central studs were not present.

Sections 2.2 and 2.3 contain a description of the design – analysis – testing iterative process that was followed in the development of these walls. The details of the construction of all test walls, including member sizes and grades, screw patterns and sizes are found at the end of Section 2.3. A description of the test setup and testing procedures is provided in Section 2.4. A discussion of the observations and measurements made during the testing phase has been provided in Section 3.

## 2.2. Predictions and numerical model

Although the conceptual configuration of the wall had been chosen, numerical analysis had to be carried out to verify the adequacy of the members. The higher resistance expected from the sheathing placement and screw size/pattern would impose greater forces on the studs compared to what would be anticipated for AISI S400 detailed walls. Furthermore, given the extent and width of the anticipated tension field force, it was necessary to consider combined axial and flexural loading on these framing members.

Since the centre-sheathed (mid-ply) configuration, as described herein, had never previously been tested, it was necessary to rely on existing design methods, valid for standard cold-formed steel shear walls, to predict the forces in the framing members. Thus, the “Effective Strip Method” from Yanagi and Yu [24] was adopted for the design process. This method to predict the width of the tension field and then to determine a corresponding ultimate resistance of a shear wall was developed for conventional single-sided walls, and calibrated against the experimental data of 70 monotonic and 72 cyclic full-scale tests of CFS sheathed shear walls by Yu et al. [4], Yu and Chen [5,6], Yu [7] and DaBreo et al. [12]. These tests covered different wall construction parameters having single-sided sheathing, using various framing thickness, sheathing thickness, fastener spacing and wall aspect ratio, all varying within specified ranges. The “Effective Strip Method” is also contained in AISI S400, for use in determining the resistance of steel sheathed CFS framed shear walls. The first centre-sheathed specimen to be tested, W18-M (Fig. 4), was designed following this method in its original form, i.e. as per Yanagi and Yu [24] and AISI S400 [1].

Knowing the spacing of the sheathing fasteners, their shear capacity

(provided by the manufacturer or calculated for tilting and bearing as per AISI S100 [25] or CSA S136 [26]), the thicknesses of the elements composing the wall and the strengths of the material used, the effective strip width ( $W_e$ ) of the tension field in the steel sheathing can be defined (Fig. 5a). With this information, as well as the aspect ratio of the wall and the resistance of an individual sheathing connection, a lateral in-plane resistance of the shear wall can be obtained. However, this method does not directly provide the specific forces in the members of the wall.

In a first attempt to determine the member loading, and to select vertical and horizontal members that can withstand the probable forces in the shear wall, a numerical SAP2000 linear elastic model was devised. The tension field of the wall was subdivided into similar independent strips matching the thickness of the sheathing (Fig. 5b). The chord stud members were defined in the model in accordance with the anticipated sections used for the experimental wall specimen and, applying the nominal shear resistance obtained from Yanagi's and Yu's method as a shear flow at the top of the model, the member forces were obtained. These values were used in comparison with the beam-column design provisions of the North American Specification for the Design of Cold-Formed Steel Structural Members [25,26]. A detailed description of the calculation and analysis process is found in the work of Brière [22] and Santos [23].

## 2.3. Iterative design process and experimental program

The behaviour exhibited by the specimens built with the centre-sheathed configuration differed from that observed for the standard CFS sheathed shear walls. The resistance achieved in the first centre-sheathed test was much higher than anticipated, which caused the frame members to fail before reaching the maximum potential of the sheathing (Fig. 6a). The new position of the sheathing relatively to the centreline of the wall had such a positive effect on the behaviour of the walls that the “Effective Strip Method” as provided by Yanagi and Yu [24] and in AISI S400 [1] could not be used in its original form to predict the shear resistance. The shear wall specimens used by Yanagi and Yu in the calibration of the “Effective Strip Method” were constructed of members with a much lower stiffness compared to the vertical and horizontal members present in the centre-sheathed configuration. Furthermore, the predicted resistance of the screw connections was limited to two-ply connections as found in AISI S100 [25] and CSA S136 [26]. The sheathing connections in the centre-sheathed wall are in contrast made of three plies, with the interior ply possessing much higher bearing capacity compared with the standard bearing

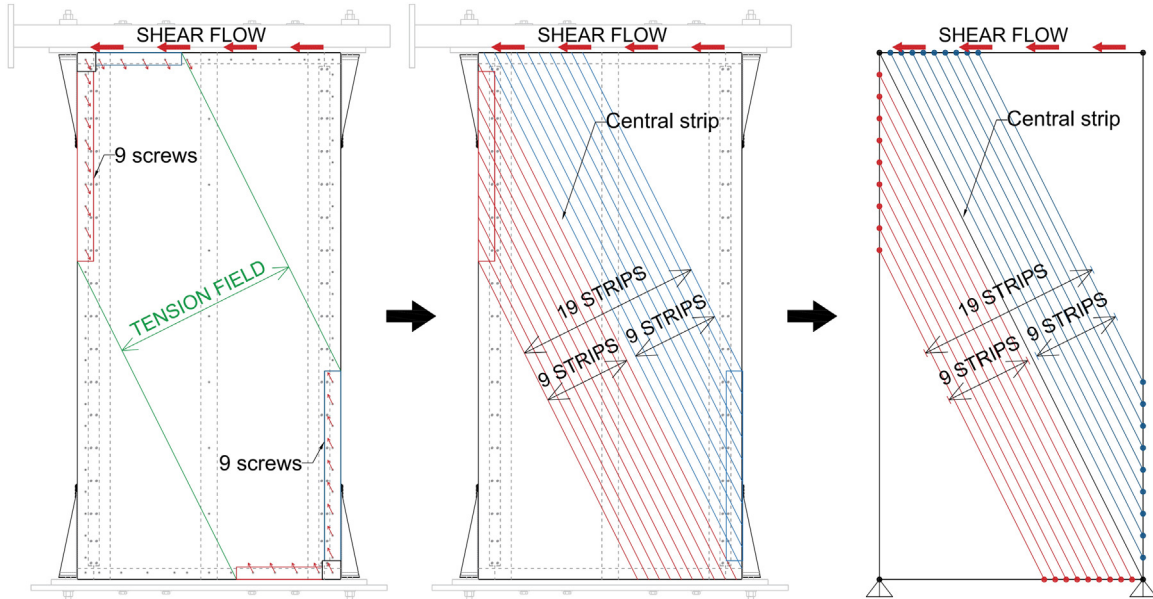


**Fig. 5.** From experimental specimen to numerical model: a) screws located within the tension field, b) equivalent strips attributed to the screw connections, and c) equivalent frame elements for the numerical model in SAP2000.

tilting resistance for screws. As such, the “Effective Strip Method” under-predicted the width of the tension field of these shear walls, as well as the force transferred within the tension field. To accommodate for this observation, a better estimate of the tension field width and force was warranted for the proper design of the chord studs.

The bearing deformations visible in the damaged sheathing of a tested specimen were a good indication of the width of the tension field (**Fig. 6c**). Their observation led to the assessment that the tension field on the centre-sheathed specimen was wider than that predicted using the “Effective Strip Method” for a wall built in this fashion. The increased width of the tension field translated into a larger number of screws participating in the shear resistance of the walls, in addition with the greater individual resistance of a fastener in the three ply scenario explained the higher shear forces carried by the wall. Thus, as a second iteration in the design and testing process, the bearing damage

pattern was used to define the new tension field width. The numerical model was revised and new forces were obtained and used for member design. This led to the requirement to reinforce the chord studs of the second shear wall test specimen. A greater lateral resistance was subsequently achieved; unfortunately, it was again much higher than anticipated due to the additionally increased stiffness of the reinforced chord stud members, which again allowed for a wider tension field and a greater number of sheathing fasteners to become engaged in resisting the lateral load (**Fig. 6b**). The subsequent post-test observations of the sheathing showed that all the screws going through the sheathing participated in carrying load; bearing damage was observed at all fastener locations. **Fig. 7** illustrates this evolution in terms of width of the tension field.

After several design - analysis - test iterations, and therefore increasing levels of reinforcement for the chord studs (**Fig. 8**), a final

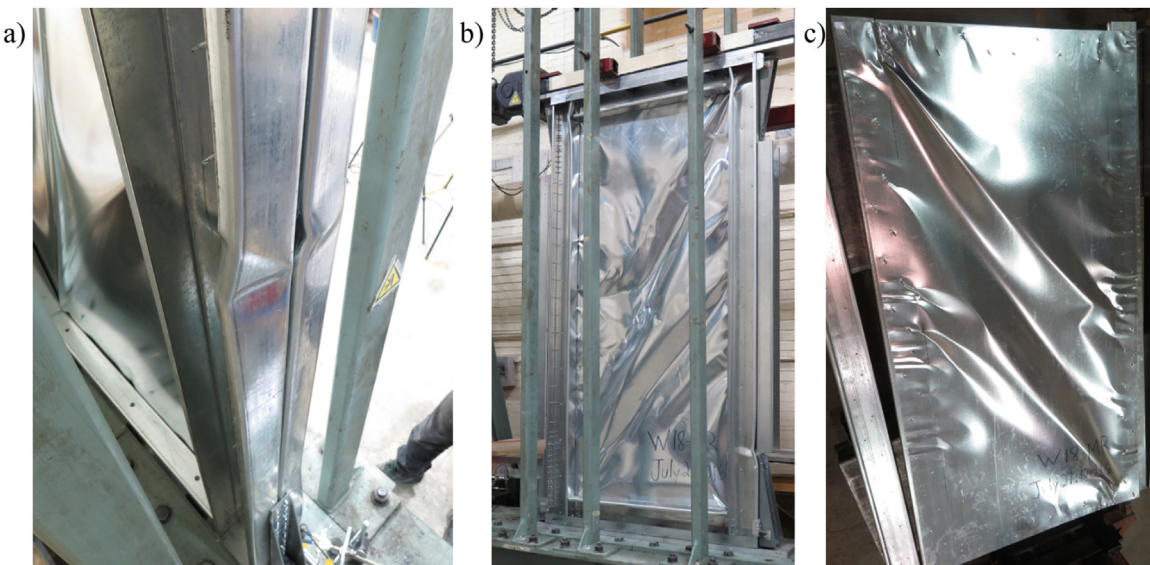


**Fig. 6.** Post-test damage chord studs and in the sheathing (used to define the width of the tension field); a) test W18-M (initial centre-sheathed wall test) showing chord stud local elastic buckling failure, b) test specimen W18-CR showing sheathing and chord stud damage, and c) test specimen W18-MR sheathing panel (removed from frame) showing tension field and bearing damage.

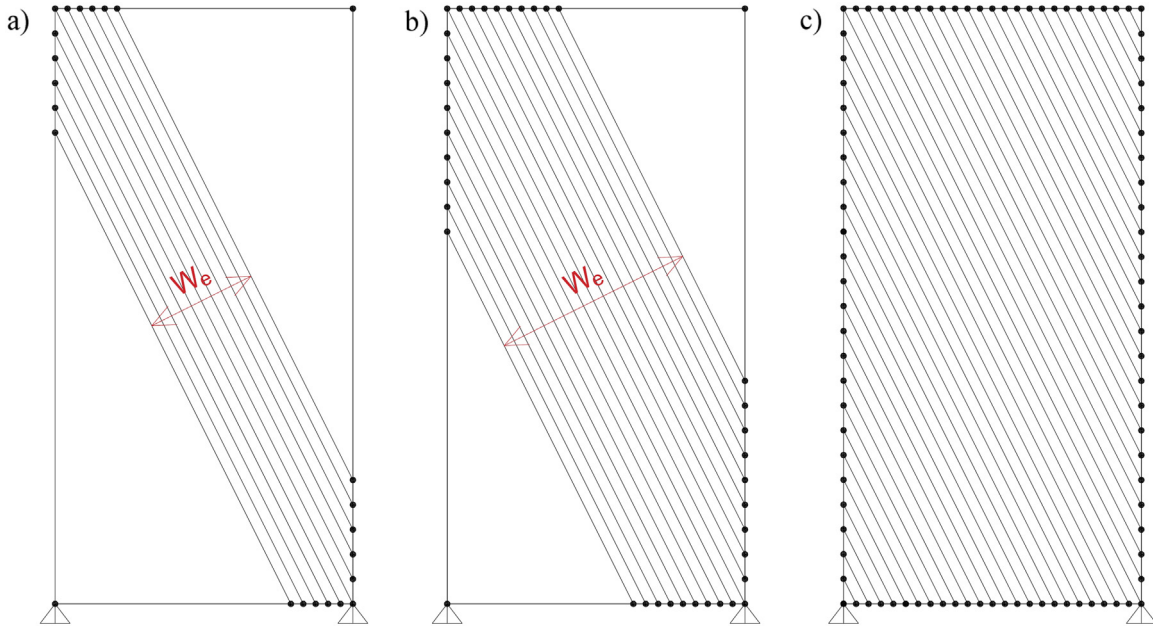


**Fig. 7.** Evolution of the “Effective Strip Method”: a) initial tension field width, b) second estimate of tension field width based on laboratory observations, and c) final estimate of the tension field width.

chord stud design was carried out assuming the participation of all the sheathing screw fasteners in resisting the lateral forces. In the decision to use the Type R3 chord stud reinforcement scheme the bearing resistance of a screw fastener was predicted using the bolt bearing resistance equation for an inside sheet of a three ply connection from Section J3.3.1 of AISI S100 [25]/CSA S136 [26]. No equivalent bearing formulation is available for three ply screw connections; historically, screws have been used in two ply connections, where both bearing and tilting of the fastener is anticipated. As an interim measure, the chord stud-to-sheathing connections were better represented by the bolt design rules; an increase of 48% in the nominal capacity of an individual

connection was calculated.

**Fig. 9** shows an elevation view and various cross-section views of the final construction details of the centre-sheathed configuration shear wall (Type R3). **Fig. 10** contains isometric illustrations of the same configuration. Details of the construction of the 15 shear wall specimen are presented in **Table 1**; 7 walls were part of the iterative design process, while the last 8 were built with the final Type R3 configuration (1 monotonic and 7 cyclic tests). Two different sheathing thicknesses were used; whereas, a single framing thickness was specified for all walls. The aspect ratio was the same for all the specimens; a length-to-height ratio of 1:2, i.e. 1218 mm × 2438 mm specimens, excluding the

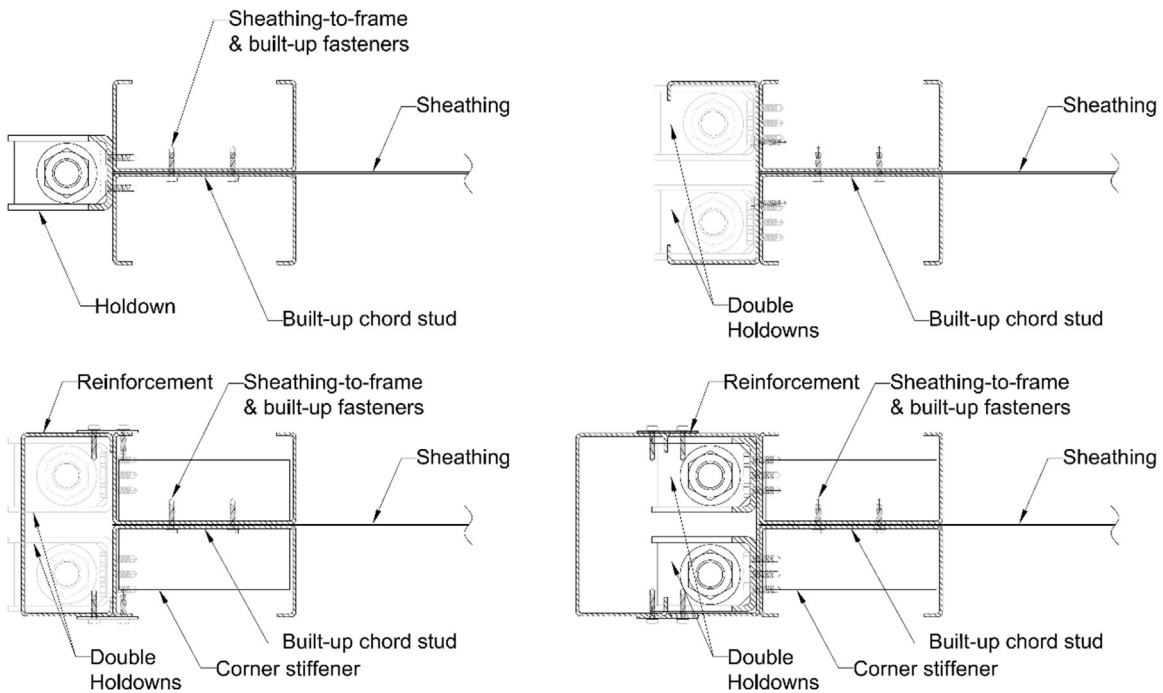


**Fig. 8.** Evolution of the chord stud reinforcement and holdown detail: a) initial configuration, b) first level of reinforcement Type R, c) second level of reinforcement Type R2, and d) final reinforcement Type R3.

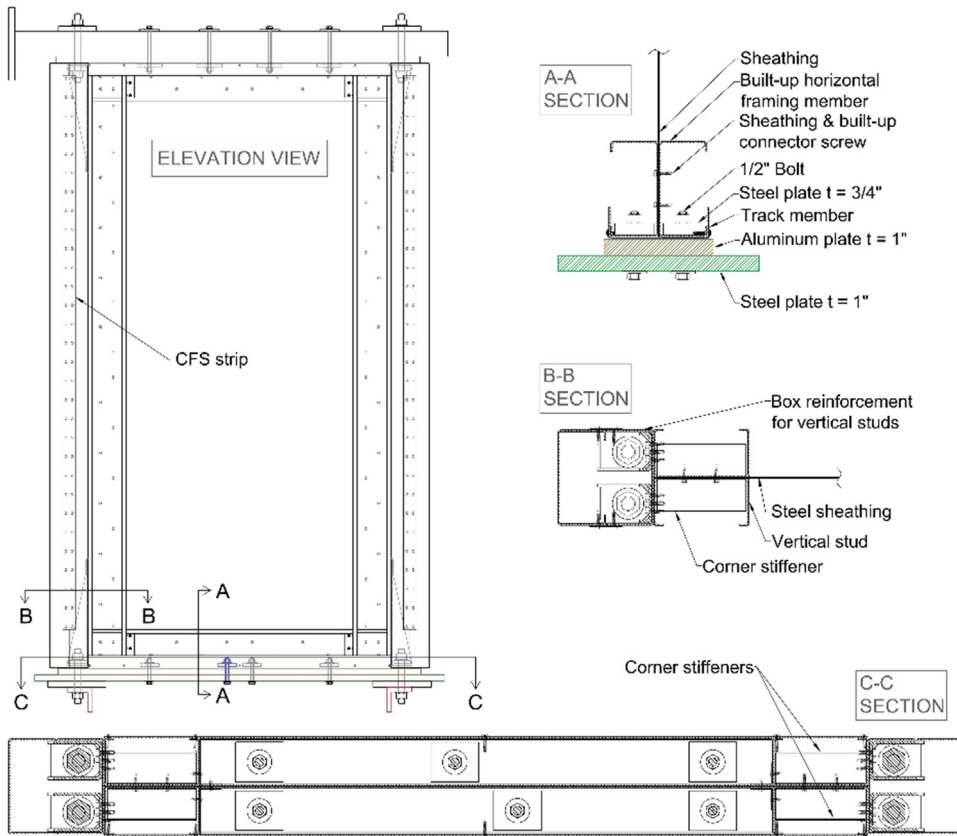


**Fig. 9.** Construction details of final centre-sheathed (mid-ply) shear wall configuration with Type R3 reinforcement scheme installed in test frame.

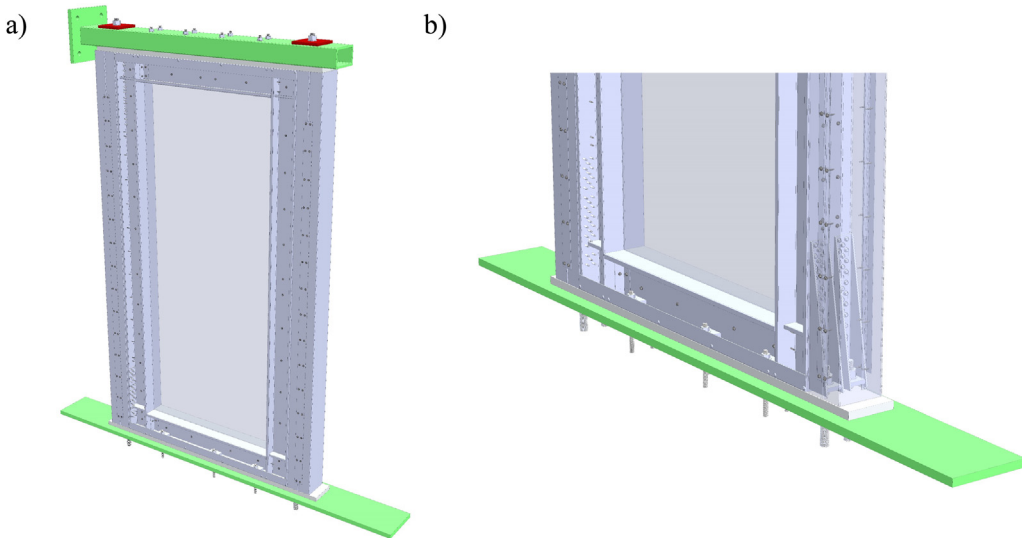


**Fig. 10.** Final centre-sheathed (mid-ply) shear wall configuration with Type R3 reinforcement installed in test frame; a) overall view, b) detailed view of base (outer chord stud reinforcement shown as transparent).

additional chord stud reinforcement. The two holdown connectors installed within the box reinforcement of each chord stud were necessary to accommodate for the uplift forces generated by the high shear resistance of the centre-sheathed configuration. The vertical and horizontal framing members, as well as the chord stud reinforcement members, were all of the same size C-section member (152.4 mm × 76.2 mm × 15.9 mm) and grade of steel (ASTM A653 Grade 340). The channel tracks were constructed of 156.0 mm × 50.8 mm members of ASTM A653 Grade 340 steel. The sheathing was obtained from ASTM A653 Grade 230 steel panels. The members used to attach the

reinforcing members were 50.8 mm wide strips, 1.73 mm in thickness, cut from ASTM A653 Grade 340 steel panels. The corner stiffeners used to reinforce the chord studs were cut from 1.73 mm thick ASTM A653 Grade 340C-section members (152.4 mm × 50.8 mm × 15.9 mm).

The holdowns were Simpson Strong-Tie S/HD15S paired with 25.4 mm ASTM A193-B7 threaded rods. Shear connectors were 12.7 mm ASTM F3125 grade A325 bolts. Hex head self-drilling/self-tapping screws were used throughout. The staggered screw pattern used to create the built-up members of the inner chord studs (Fig. 9) was necessary since these screws fastened the sheathing and also connected

**Table 1**

Centre-sheathed (mid-ply) shear wall test program: list of shear wall configurations, components and test protocol.

Test ID	Sheathing thickness (mm)	Framing thickness (mm)	Sheathing screw size (#)	Fastener spacing (mm)	Type of test <sup>a</sup>
W15	0.84	2.46	10	50	M_R3 & C_R3
W16	0.84	2.46	10	50	M_R & M_R2
W17	0.84	2.46	10	150	M & C
W18	0.84	2.46	10	100	M, M_R & C_R
W23	1.09	2.46	12	100	C_R3
W24	1.09	2.46	12	150	C_R3
W25 <sup>b</sup>	0.84	2.46	10	100	C_R3
W26 <sup>b</sup>	1.09	2.46	10	100	C_R3
W15B <sup>b</sup>	0.84	2.46	10	50	C_R3
W23B <sup>b</sup>	1.09	2.46	12	100	C_R3

<sup>a</sup> M: Monotonic; C: Cyclic; \_R, \_R2 and \_R3: Different frame reinforcement scheme (Fig. 8).

<sup>b</sup> Asymmetric cyclic test to reach a higher maximum chord rotation.

the members of the built-up chord stud. The associated screw spacing is taken as the vertical (horizontal) distance between two screws of the chord studs (resp. horizontal framing members). Corner stiffeners were added inside the ends of the chord studs (Section B-B and C-C in Fig. 9) to reduce the damage at the wall corners due to the contact between the vertical and horizontal frame members when experiencing high chord rotation. A complete description of each test specimen with detailed drawings can be found in the theses of Brière [22] and Santos [23].

#### 2.4. Test setup and testing procedures

All shear wall specimens were assembled in the Jamieson Structures Laboratory at McGill University, with the appropriate holes pre-drilled in the horizontal framing and track members to accept the required shear and holdown anchors. Each wall was installed in the specifically constructed reaction frame for the testing of CFS walls (Fig. 11). It consists of a 250 kN capacity actuator having a displacement range of  $\pm 125$  mm. Lateral bracing at the wall top ensured that only in-plane deformation of the wall specimen took place. LVDTs and string potentiometers were installed to record the in-plane deformations of the test wall, including; slip, uplift and top of wall displacement. The uplift measurements were obtained at the base of the chord studs, and as such

included the vertical displacement of the holdowns. The measurement instruments were connected to Vishay Model 5100B scanners which were used to record data using the Vishay System 5000 StrainSmart software.

The specimens were tested using three different displacement based loading protocols: monotonic, symmetric cyclic and asymmetric cyclic. The monotonic protocol was set at a rate of 5.0 mm/min. The symmetric cyclic protocol followed the CUREE (Consortium of Universities for Research in Earthquake Engineering) reversed cyclic protocol [27,28]. Due to the increased ductility of the specimens built following the centre-sheathed configuration, and the limited range of the actuator, an asymmetric cyclic protocol was also used in which the CUREE defined displacements were applied in a single direction to capture the degradation in strength at large shear deformations. A displacement rate of 0.05 Hz was applied for the symmetric cyclic protocol and for cycles below 125 mm in the asymmetric protocol; a rate of 0.025 Hz was used thereafter. Detailed loading protocol information is provided in the theses of Brière [22] and Santos [23].

#### 3. Test results and observations of Type R3 reinforced shear walls

Presented herein are the general test results and observations of the centre-sheathed shear walls constructed with the Type R3 chord stud reinforcement. Under lateral in-plane load these walls experienced shear buckling of the sheathing, the development of a tension field in the panel and bearing deformations of the sheathing (Fig. 12). Given the high axial forces (tension and compression) in the chord studs, minor uplift displacements were also observed during loading. The ductile energy dissipating mechanism of these shear walls is facilitated by the steel bearing deformations in the confined sheathing (Fig. 13b). This deformation is far more extensive than that observed in walls where the sheathing is placed on the exterior of the frame (Fig. 13a), for which the panel can disengage from the wall. The vertical and horizontal framing members remained largely undamaged (Fig. 14) during loading; the minor deformations seen in Fig. 14b are due to the extensive drift rotations of these walls, which in the best cases exceeded 6%. Fig. 15 shows a representative monotonic/cyclic backbone curve and illustrates the measured properties obtained from each test (Table 2). The results were computed using the average of the ultimate resistances  $S_u$ , and associated displacements  $\theta_u$ , also expressed as a drift ratio, from the positive and negative ranges of the symmetric cyclic tests. For the single monotonic test and the asymmetric cyclic tests, the values were taken from the positive range only. The total energy dissipated,  $E_{TOT}$ , during a test is represented by the sum of the areas comprised within the force-deformation curve of each cycle. Thus, the total cumulative energy, obtained using an incremental approach, was computed using the complete set of data coming from the cyclic tests, without differentiating the energies cumulated during a positive or a negative displacement.

Of the eight Type R3 reinforcement shear walls, the strongest was W15B-CR3, which reached a maximum shear resistance of 165.7 kN/m at a lateral displacement of 160 mm (drift of 6.56%). Test W15-CR3 was of the exact same construction, however during the symmetric cyclic loading the stroke of the actuator was insufficient for the wall to reach its ultimate shear resistance even through drift rotations of above 4% were reached (Fig. 16). Hence, this wall was retested under the asymmetric cyclic loading protocol (Fig. 17), during which these maximum results were measured. Specimen W15B-CR3 experienced an onset of strength degradation after reaching a lateral displacement of 180 mm (drift of 7.4%). The increase in shear resistance near the zero displacement point in a return cycle of the asymmetric test (Fig. 17) was the result of reduced slotting (bearing deformation) in the sheathing because the walls did not undergo full reversed cycles.

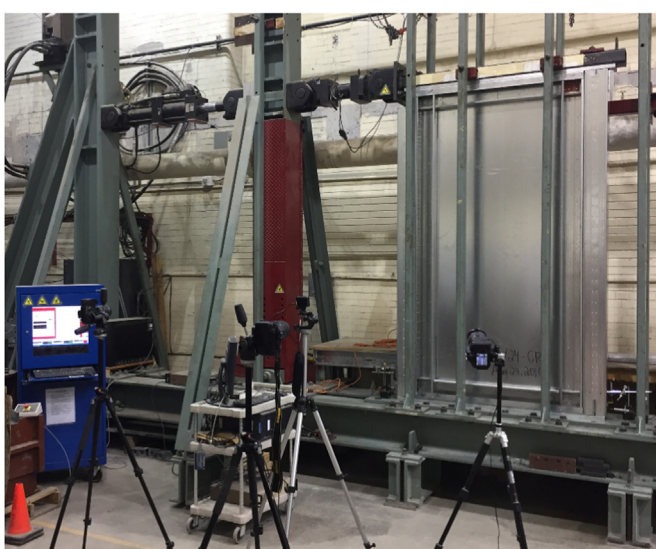
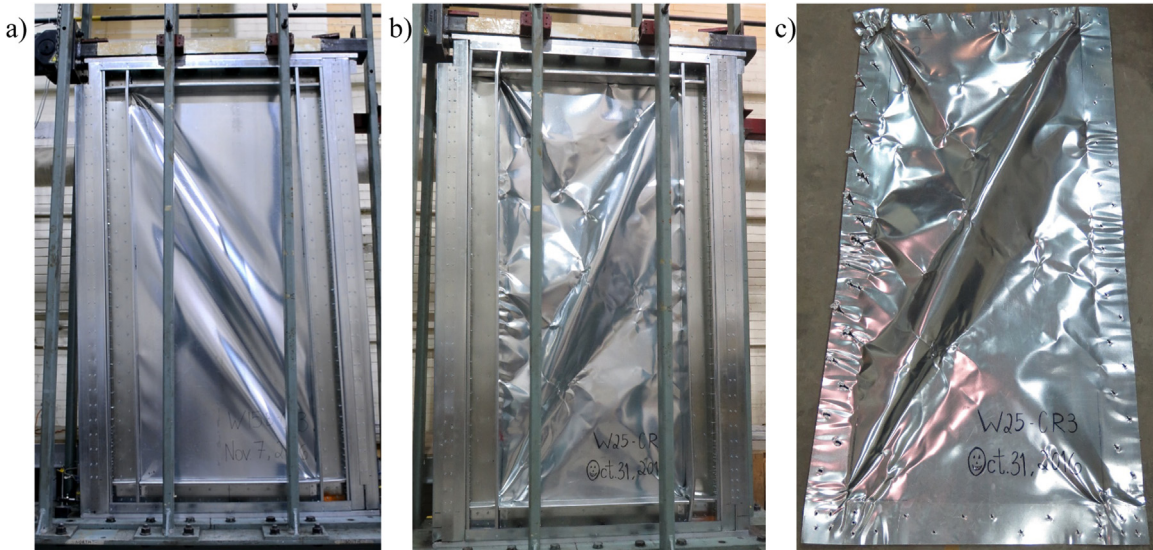


Fig. 11. Shear wall test setup.



**Fig. 12.** Photographs of shear wall specimen; a) W15B-CR3 under load showing shear buckling and tension field in sheathing, b) W25-CR3 post-test showing framing members in good condition, and c) W25-CR3 showing damage largely confined to the bearing/slotted of sheathing.

#### 4. Influence of the construction parameters

The Type R3 centre-sheathed specimens were tested using different construction parameters; sheathing thickness, screw spacing and screw size (Table 1). The choice of these parameter did have a direct influence on the ultimate shear strength, as well as the extent of strength degradation occurring during the tests; nonetheless, the general behaviour of the shear wall specimens remained consistent as described in Section 3.

The use of a thicker sheathing member resulted in an increase of the ultimate shear strength of the shear wall (Fig. 18). As the major part of the shear resistance comes from the bearing strength of the sheathing screw connections, the increase of the sheathing thickness resulted in a higher shear strength; indeed, the bearing strength for each connection is directly related to the thickness of the material. Similarly, increasing the diameter of the sheathing screws resulted in an increased ultimate shear strength of the wall, as well as a better overall ductility (Fig. 19); as the bearing strength of a screw connection is also directly related to the diameter of the fastener. Reducing the screw spacing also increased the ultimate shear resistance of the centre-sheathed wall specimens (Fig. 20). The sheathing screws are the essential elements used for transferring the lateral shear force applied at the top of the wall through the sheathing; therefore reducing the sheathing screw spacing (i.e. increasing the number of sheathing screws) resulted in an increase of the ultimate strength and the ductility of the specimens.

However, it is important to note that moving from a #10 to #12 screw size, while increasing the screw spacing, although possibly attractive because it requires less labour for construction, did not result in an advantage based on structural performance. The sheathing screws

have a dual responsibility in the centre-sheathed wall. They allow for the transfer of in-plane shear loads through the wall, and they create the fixity for the built-up chord studs. The larger screw spacing pattern (150 mm) did not provide for adequate connection of the two main C-Sections of the chord studs, and allowed for them to separate under loading, which led to the earlier onset of shear force degradation in the wall. This can also be seen in terms of ductile behaviour of the two centre-sheathed specimens W23-CR3 and W24-CR3 which were constructed with #10 screws, but at different spacing, 100 mm and 150 mm, respectively. A degradation in shear strength was observed for W24-CR3 after 80 mm lateral displacement applied at the top of the wall, whereas for W23-CR3, constructed with a smaller screw spacing, was able to maintain its shear resistance and the connectivity of the built-up chord studs throughout the symmetric cyclic test protocol. It is the large out-of-plane force associated with the shear buckling of the confined sheathing that causes the individual C-Section chord studs to separate from one another, and the wall to then lose capacity.

#### 5. Evaluation of shear resistance using an equivalent energy approach

Cold-formed steel sheathed shear walls exhibit a nonlinear force - deformation behaviour; the innovative configurations tested for this study did not behave otherwise. As for the previous experimental programs, summarized by DaBreo et al. [12], relied on to develop the Canadian shear wall design method [13] found in AISI S400 [1], the Equivalent Energy Elastic Plastic (EEEP) method [29,30] was used to describe the behaviour of the specimens with a bilinear elastic-plastic curve and to evaluate design properties such as the yield force, stiffness

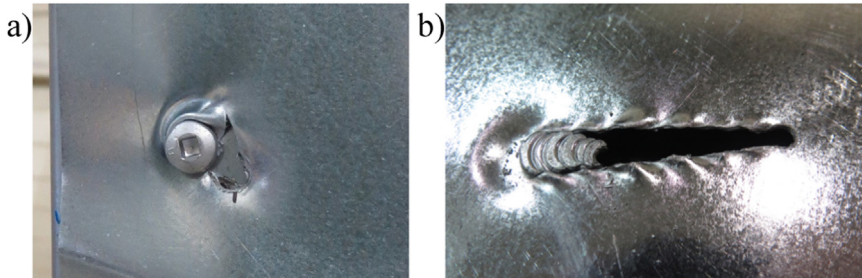


**Fig. 13.** Post-test photographs bearing damage in sheathing; a) panel placed on exterior of wall, and b) panel confined between framing members.

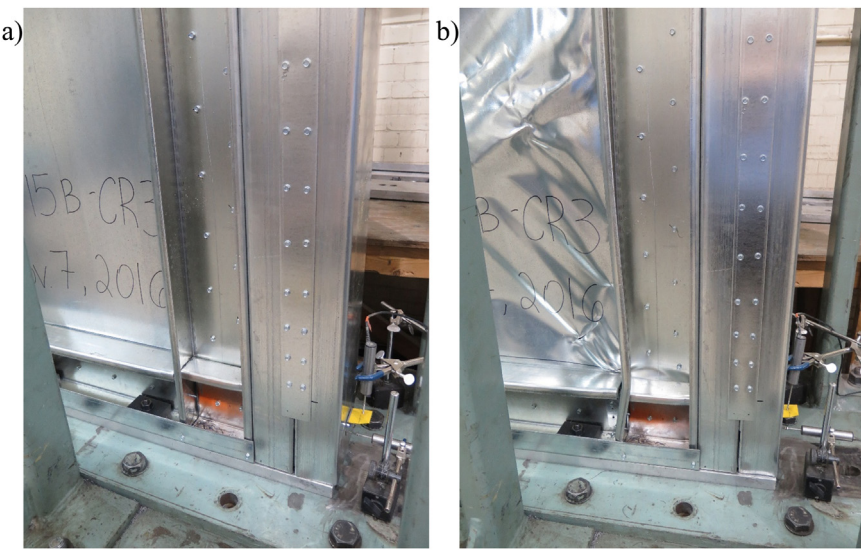


Fig. 14. Photographs of test W15B-CR3; a) prior to test, and b) post-test.

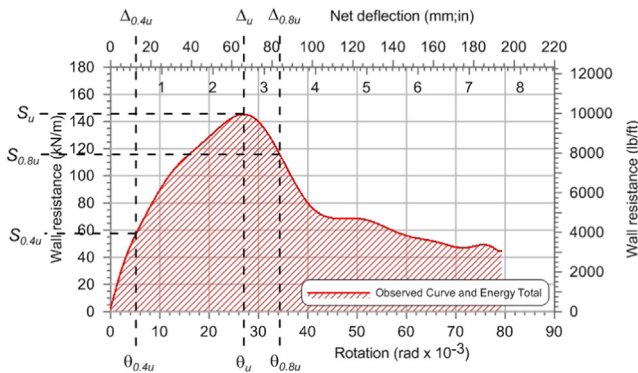


Fig. 15. Graphic representation of the parameters included in test results.

and ductility. Indeed, Branston et al. [31,32] showed that the EEEP model best represented the behaviour of cold-formed steel framed - wood sheathed shear walls tested using monotonic and reversed cyclic loading protocols. This analysis approach has been used in the development of both the Canadian design method in AISI S400 for structural wood panel and steel panel sheathed CFS shear walls. As such, it was implemented in this study to provide information consistent with that available for CFS shear walls with steel sheathing installed on the exterior of the framing.

This analysis method relies on the idea that the energy dissipated during a test (monotonic or cyclic) is represented by the area under the

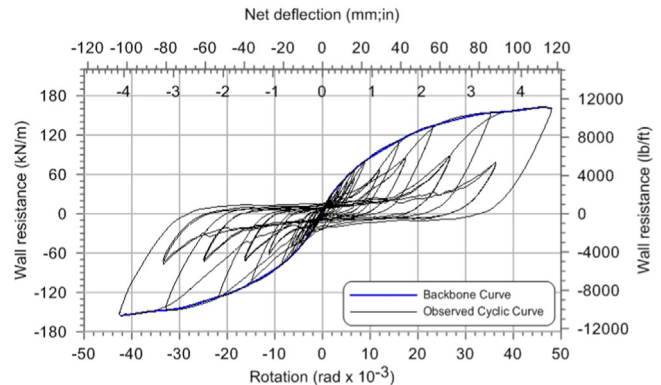


Fig. 16. Shear wall resistance versus rotation for Specimen W15-CR3 – symmetric cyclic loading.

force-displacement curve, which is also equal to the energy represented by the area under the bilinear curve obtained using the EEEP method (Fig. 21). The energy considered here is the energy dissipated by the specimen until reaching 80% of the ultimate load after the latter had been obtained; once this post-peak load is reached, failure of the specimen (ultimate displacement) is considered to have occurred. Therefore, the highly nonlinear behaviour of the specimen is transformed into a perfectly elastic/plastic behaviour dissipating the same amount of energy within this defined range. The main parameters necessary to create the EEEP curve are the ultimate wall resistance,  $S_u$ , the wall

**Table 2**  
Measured properties of test walls constructed with the final reinforcement scheme (Type R3).

Test ID	Ultimate Resistance $S_{u,\text{avg}}$ (kN/m)	Displacement at $S_u$ $\Delta_{u,\text{avg}}$ (mm)	Displacement at $0.4S_u$ $\Delta_{0.4u,\text{avg}}$ (mm)	Drift Ratio at $S_u(\%)$	Drift Ratio at $0.4S_u(\%)$	Total Energy Dissipated $E_{\text{TOT}}$ (J)
W15-MR3	149.8	119.9	14.7	4.92	0.60	16,788
W15-CR3 <sup>a</sup>	158.9	107.5	15.2	4.41	0.63	75,743
W15B-CR3 <sup>b</sup>	165.7	160.0	13.3	6.56	0.55	109,013
W23-CR3 <sup>a,c</sup>	162.5	120.4	15.1	4.94	0.62	48,419
W23B-CR3 <sup>b</sup>	158.6	121.6	14.0	4.99	0.57	98,377
W24-CR3 <sup>a</sup>	131.4	79.6	12.7	3.26	0.52	76,112
W25-CR3 <sup>b</sup>	116.7	86.0	12.7	3.53	0.52	70,483
W26-CR3 <sup>b</sup>	145.3	65.7	12.9	2.70	0.53	61,059

<sup>a</sup> Symmetric cyclic tests.

<sup>b</sup> Asymmetric cyclic test to reach a higher maximum chord rotation.

<sup>c</sup> Protocol stopped during test; negative cycles not completed. Results for positive cycles only.

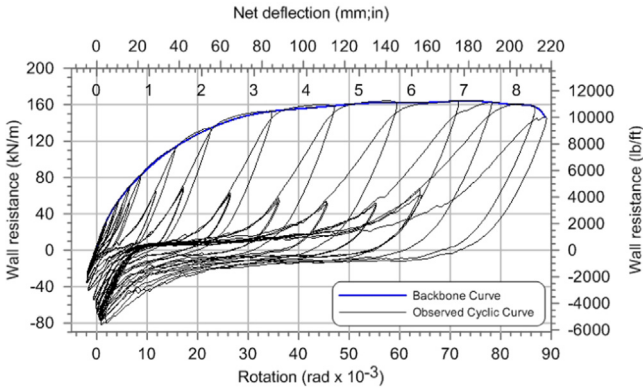


Fig. 17. Shear wall resistance versus rotation for Specimen W15B-CR3 – asymmetric cyclic loading.

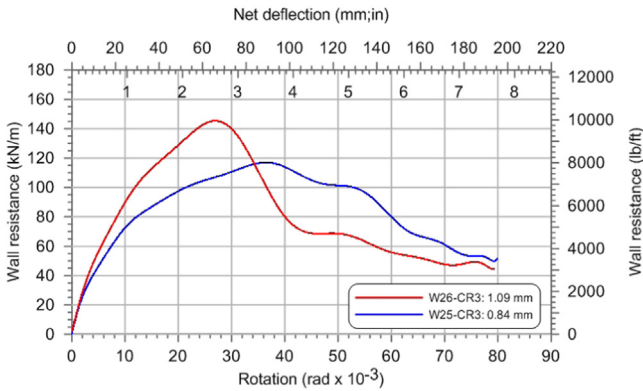


Fig. 18. Test results from two similar specimens using different sheathing thicknesses.

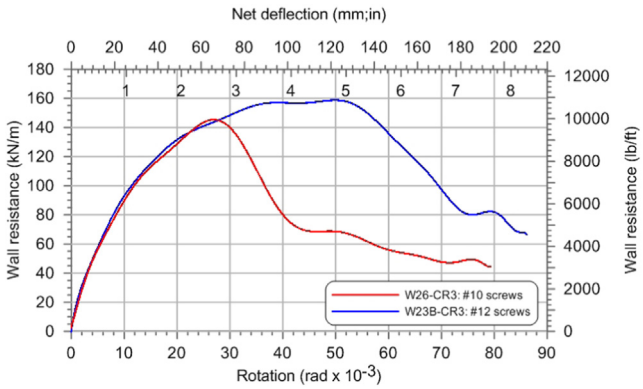


Fig. 19. Test results from two similar specimens using different screw sizes.

resistance at 80% of  $S_u$  post-peak,  $S_{0.8u}$ , the wall resistance at 40% of  $S_u$  pre-peak,  $S_{0.4u}$ , and their respective displacements  $\Delta_u$ ,  $\Delta_{0.8u}$  and  $\Delta_{0.4u}$  (Fig. 21). Note, given the extended drift that many of the centre-sheathed walls achieved, the post-peak displacement at 4% drift was defined as the value for  $\Delta_{0.8u}$  in walls which were able to displace past this point. This choice was made in consideration of the 2.5% inelastic drift limit found for seismic design in the National Building Code of Canada [33] and ASCE 7 [34]; depending on shear strengths reached at drifts beyond 4% would be unrealistic for design. Example analyses are shown in Fig. 22. Shear resistance predictions using the EEEP approach are also provided in Section 6.

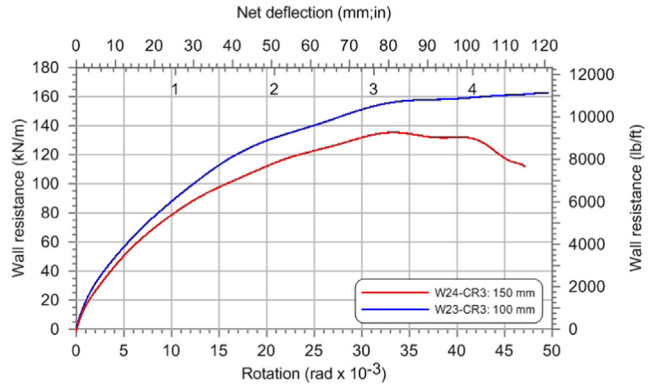


Fig. 20. Test results from two similar specimens using different screw spacing.

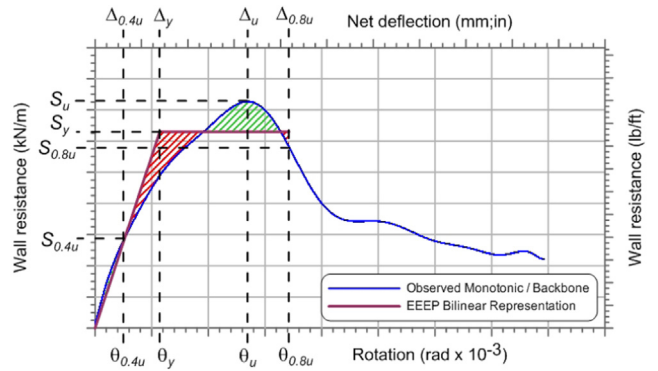


Fig. 21. Equivalent Energy Elastic-Plastic (EEEP) bilinear model.

## 6. Preliminary design procedure for centre-sheathed (mid-ply) shear walls

The iterative design process utilized to develop the centre-sheathed shear wall demonstrated that the “Effective Strip Method” as per Yanagi and Yu [24] and the AISI S400 Standard [1] is not adequate for the design of this specific type of lateral system. It was necessary to adapt the tension field analysis approach based on the observations that were made during laboratory testing. Two assumptions were made during the iterative design process; 1) all the sheathing screws are considered to participate in the shear resistance of the walls, and 2) each fastener is able to reach a bearing resistance computed considering the interior ply double shear bolt bearing capacity from Section J3.3.1 of AISI S100 [25]/CSA S136 [26]. Fig. 23 illustrates the bearing forces at fastener locations on one end of the tension field as they were considered in the calculation of the nominal shear resistance of the test walls. Note, only half of the sheathing fasteners are depicted under load; the other half of the screws represents the opposite anchor for the tension field.

The nominal shear resistance (force per unit length) predicted for a centre-sheathed configuration specimen as per the preliminary “Modified Effective Strip Method”,  $S_{n(MESM)}$ , is given by Eq. (1).

$$S_{n(MESM)} = \left( \frac{n}{2} \times P_{nb} \times \cos \alpha \right) / w \quad (1)$$

where,

- $n$ = Total number of sheathing screws of the wall;
- $P_{nb}$ = Screw fastener's nominal bearing capacity as per Section J3.3.1 [25,26];
- $\alpha$ = Angle given by the aspect ratio of the wall (Fig. 23);
- $w$ = Length of the wall.

The ultimate shear resistance of the centre-sheathed configuration

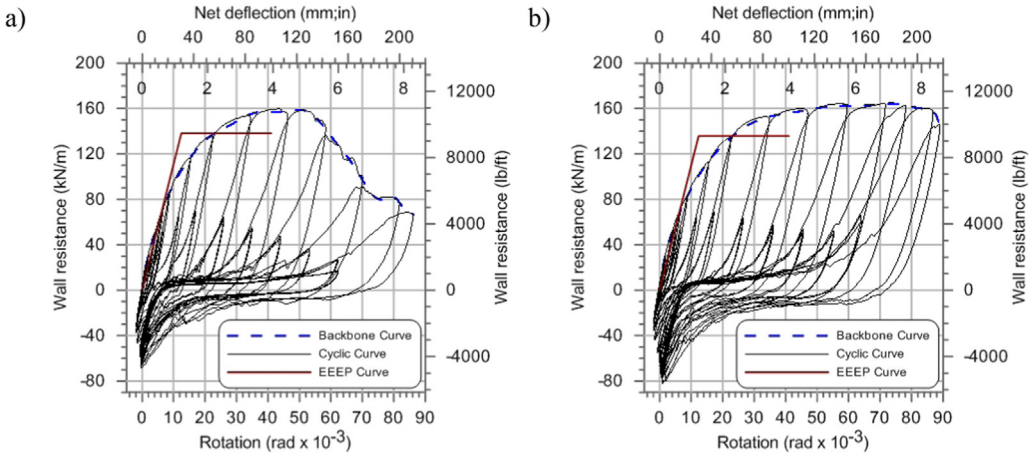


**Fig. 22.** Shear wall resistance versus rotation with superimposed EEEP bilinear curve; a) Specimen W23B-CR3 (asymmetric cyclic loading), and b) Specimen W15B-CR3 (asymmetric cyclic loading).

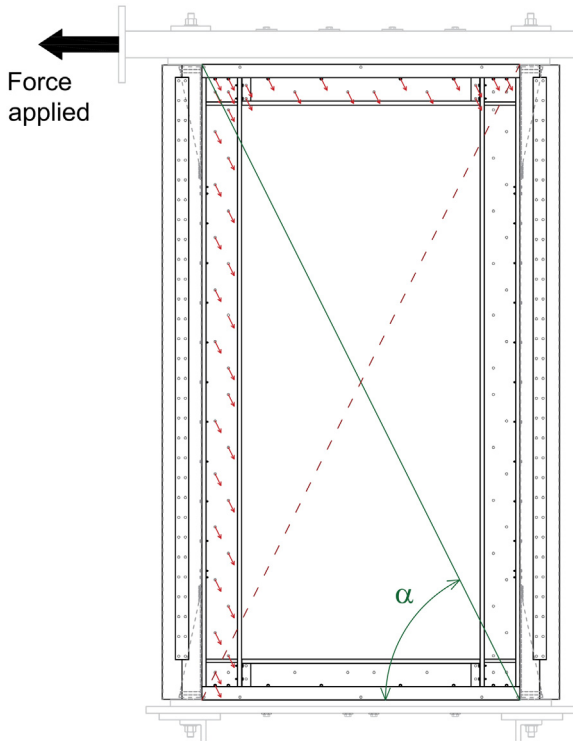


**Fig. 23.** Bearing strength and screws participating for a centre-sheathed configuration specimen.

specimens was reached at drift ratios ranging from 2.7% (65.7 mm for the positive cycles of W26-CR3) to 6.6% (160 mm) for the positive cycles of W15B-CR3; these displacements are too large to be considered in design given the typical seismic inelastic drift limits. It was decided to use the 2.5% inelastic storey-drift limit criterion for seismic design of the NBCC [33] and ASCE/SEI 7 [34], considering the shear resistance exhibited at that displacement for the design. For comparison purposes, the ratios of test-to-predicted resistance were computed taking the average ultimate shear resistance,  $S_{u,\text{avg}}$ , and the average measured shear resistance at the 2.5% drift level,  $S_{2.5\%,\text{avg}}$ , as the test values. They were compared with the average shear resistance obtained with the EEEP method,  $S_{y,\text{avg}}$ , and the shear resistance obtained with the preliminary "Modified Effective Strip Method",  $S_{n(\text{MESM})}$ , in order to compute the test-to-predicted ratios for the Type R3 walls in Table 3.

Comparing the shear resistances obtained at 2.5% drift with the

values obtained applying the EEEP analysis method on the test results confirms the consistency in considering the shear resistance at 2.5% drift for design. Although specimen W26-CR3 presents a ratio  $S_{2.5\%}/S_y$  slightly superior to the others, the mean value for this ratio is 1.04, with a standard deviation of 0.043 and a coefficient of variation of 4.1%. The ratios considering  $S_u$  are not used since the range of displacement within which it is achieved is too large (2.7–6.6% drift). However, the mean of 1.07 with a standard deviation of 0.092 and a coefficient of variation of 8.6% for the ratio  $S_u/S_{n(\text{MESM})}$  attest to the assumptions made in the definition of the prediction method.

The ratio  $S_{2.5\%}/S_{n(\text{MESM})}$  was selected for the design method since the shear flow at that displacement was shown to be a consistent value. The mean of 0.98 is close to unity, but the standard deviation and coefficient of variation of 0.107% and 10.9% respectively enlighten the fact that the prediction method needs to be further optimized to consider all the parameters affecting the shear resistance of a centre-sheathed configuration test specimen. Further study is needed on the three ply bearing resistance of screw connections, beyond simply assuming that the bolt bearing rules in AISI S100 and CSA S136 are transferable. Furthermore, given the reliance of the width of the tension field on the relative stiffness of the framing members, guidance is needed with respect to the minimum framing stiffness needed to utilize the entire width of the sheathing panel, and how to link with the "Effective Strip Method" by Yanagi and Yu, which has been proven to provide accurate shear resistance values for the more flexible single-sided shear walls.

## 7. Conclusions

An innovative centre-sheathed (mid-ply) shear wall configuration was developed in the pursuit of using CFS framed construction for mid-rise buildings. This configuration allowed for the concentric placement of the sheathing, which was confined between the built-up vertical and horizontal framing members. This minimized torsional loading on the framing members, provided for the opportunity to use thicker sheathing with better performing sheathing connections, and allowed for a substantial increase in both the shear resistance and ductility of CFS shear walls. The final configuration was developed through an iterative design – analysis – testing process due to the lack of an appropriate design procedure prior to launching this study. It was observed that the existing "Effective Strip Method" by Yanagi and Yu and contained in AISI S400, although adequate for the single-sided shear walls constructed as per the configurations that were used in its calibration, is not satisfactory for the design of these new centre-sheathed walls. The tension field encompasses the entire sheathing member, and the bearing resistance of the middle ply in a three ply sheathing connection is substantially

**Table 3**

Comparison of prediction methods with measured shear resistance for cyclic Type CR3 walls.

Test ID	Average Test Values (kN/m)		Predicted Values (kN/m)		Ratios Test/Predicted			
	S <sub>u,avg</sub>	S <sub>2.5%,avg</sub>	S <sub>y,avg</sub> (EEEP)	S <sub>n(MESM)</sub>	S <sub>u/S<sub>y</sub></sub>	S <sub>u/S<sub>n(MESM)</sub></sub>	S <sub>2.5%/S<sub>y</sub></sub>	S <sub>2.5%/S<sub>n(MESM)</sub></sub>
W15-R3 <sup>a</sup>	154.3	135.2	131.2	161.8	1.18	0.95	1.03	0.84
W15B-CR3 <sup>c</sup>	165.7	141.3	136.4	161.8	1.21	1.02	1.04	0.87
W23-CR3 <sup>b,d</sup>	162.5	140.1	138.9	149.8	1.06	0.98	1.01	0.94
W23B-CR3 <sup>c</sup>	158.6	140.8	138.1	149.8	1.15	1.06	1.02	0.94
W24-CR3 <sup>b</sup>	131.4	121.5	115.8	115.8	1.13	1.13	1.05	1.05
W25-CR3 <sup>c</sup>	116.7	106.0	102.8	95.7	1.14	1.22	1.03	1.11
W26-CR3 <sup>c</sup>	145.3	143.3	126.0	132.1	1.15	1.10	1.14	1.09
			Avg.	1.15	1.07	1.04	0.98	
			Std. Dev.	0.047	0.092	0.043	0.107	
			Coeff. of Var.	4.1%	8.6%	4.1%	10.9%	

<sup>a</sup> Average value from cyclic and monotonic tests.<sup>b</sup> Average value from reversed cyclic tests only.<sup>c</sup> Positive values from asymmetric cyclic tests only.<sup>d</sup> Negative cycles incomplete; positive range considered.

higher than that predicted using the screw bearing/tilting design rules found in AISI S100 and CSA S136.

The shear resistance of a specimen was influenced by the building parameters with which it was built, i.e. thicker sheathing, larger screws and smaller screw spacing provided higher shear strength. However, these parameters had to be contained within a certain range; the actuator's capacity, as well as the resistance of the chord studs facing high axial compressive force and bending moment imposed an upper limit to the potential shear strength of the specimens. In addition, the screw spacing had to be limited on the other end of the range as well; too large of a screw spacing would result in the separation of the built-up chord stud due to a large out-of-plane force caused by the shear buckling of the sheathing.

Performance-wise, the centre-sheathed configuration presented the advantage of confining the panel between the framing members preventing it from detaching from the screw fasteners when slotted holes appeared in the panels. This allowed for full use of the extensive bearing failure mechanism. The strongest specimen from the centre-sheathed configuration achieved an ultimate shear resistance of 165.7 kN/m, more than four times what is currently available for design in AISI S400, at a drift rotation superior to 6%.

The centre-sheathed shear wall represents a new category of CFS lateral system in terms of its vastly improved resistance and ductility; its measured response to load illustrates the potential to be integrated in the construction of mid-rise buildings. However, certain aspects are at the primary stage of understanding; further research is needed to obtain a more complete range of shear resistance properties having the same level of ductility, i.e. from the current maximum shear strength listed in AISI S400 to what was tested as part of this study. Furthermore, an investigation into the bearing resistance of three ply screw connections is warranted, as is the development of a method to relate the effective width of the tension field in the sheathing with the relative stiffness of the framing members. Lastly, the wall specimens described in this paper were all of a 1:2 aspect ratio with general dimensions of 1218 mm × 2438 mm. As such, comments as to the impact of the aspect ratio or the general geometry of the centre-sheathed shear wall cannot be presented at this time. Research is ongoing to address these identified shortcomings of the study described herein.

## Acknowledgements

Financial support for this research was provided by the American Iron and Steel Institute (AISI), the Canadian Sheet Steel Building Institute (CSSBI) and the Natural Sciences and Engineering Research Council of Canada (NSERC) (Grant no.CRDP J 479638-15). The materials and tools for construction of the test specimens were provided by

Bailey Metal Products Ltd., Simpson Strong-Tie Company Inc., Ontario Tools & Fasteners Ltd., UCAN and Arcelor Mittal.

A special thank you is extended to Robert Rizk, Andrea Iachetta and Keith Lee; the laboratory phase of the research would not have been possible without the support of these students.

## References

- [1] American Iron and Steel Institute (AISI). North American standard for seismic design of cold-formed steel structural systems. AISI S400-15. Washington, USA; 2015.
- [2] Serrette RL, Nguyen H, Hall G. Shear wall values for light weight steel framing. Report no. LGSRG-3-96. Santa Clara, USA: Dept. of Civil Engineering, Santa Clara University; 1996.
- [3] Serrette RL, Encalada J, Matchen B, Nguyen H, Williams A. Additional shear wall values for light weight steel framing. Report no. LGSRG-1-97. Santa Clara, USA: Dept. of Civil Engineering, Santa Clara University; 1997.
- [4] Yu C, Vora H, Dainard T, Tucker J, Veetvarki P. Steel sheet sheathing options for cold-formed steel framed shear wall assemblies providing shear resistance, Report no. UNT-G76234. Denton, USA: Dept. of Engineering Technology, University of North Texas; 2007.
- [5] Yu C, Chen Y. Steel sheet sheathing options for cold-formed steel framed shear wall assemblies providing shear resistance – phase 2. Report no. UNT-G70752. Denton, USA: Dept. of Engineering Technology, University of North Texas; 2009.
- [6] Yu C, Chen Y. Detailing recommendations for 1.83 m wide cold-formed steel shear walls with steel sheathing. J Constr Steel Res 2011;67(1):93–101.
- [7] Yu C. Shear resistance of cold-formed steel framed shear walls with 0.686 mm, 0.762 mm, and 0.838 mm steel sheet sheathing. Eng Struct 2010;32(6):1522–9.
- [8] Ellis J. Shear resistance of cold-formed steel framed shear wall assemblies using CUREE test protocol. Anaheim, USA: Simpson Strong-Tie Co. Inc.; 2007.
- [9] Shamim I, DaBreo J, Rogers CA. Dynamic testing of single- and double-story steel-sheathed cold-formed steel-framed shear walls. ASCE J Struct Eng 2013;139:807–17.
- [10] Shamim I, Rogers CA. Steel sheathed/CFS framed shear walls under dynamic loading: numerical modelling and calibration. Thin-Walled Struct 2013;71:57–71.
- [11] Shamim I, Rogers CA. Numerical evaluation: AISI S400 steel-sheathed CFS framed shear wall seismic design method. Thin-Walled Struct 2015;95:48–59.
- [12] DaBreo J, Balh N, Ong-Tone C, Rogers CA. Steel sheathed cold-formed steel framed shear walls subjected to lateral and gravity loading. Thin-Walled Struct 2013;74:232–45.
- [13] Balh N, DaBreo J, Ong-Tone C, El-Saloussy K, Yu C, Rogers CA. Design of steel sheathed cold-formed steel framed shear walls. Thin-Walled Struct 2014;75:76–86.
- [14] Xie Z, Yan W, Yu C, Mu T, Song L. Experimental investigation of cold-formed steel shear walls with self-piercing riveted connections. Thin-Walled Struct 2018;131:1–15.
- [15] Attari NKA, Alizadeh S, Hadidi S. Investigation of CFS shear walls with one and two-sided steel sheeting. J Constr Steel Res 2016;122:292–307.
- [16] Javaheri-Tafti MR, Ronagh HR, Behnamfar F, Memarzadeh P. An experimental investigation on the seismic behavior of cold-formed steel walls sheathed by thin steel plates. Thin-Walled Struct 2014;80:66–79.
- [17] Tian H-W, Li Y-Q, Yu C. Testing of steel sheathed cold-formed steel trussed shear walls. Thin-Walled Struct 2015;94:280–92.
- [18] Zhang W, Mahdavian M, Li Y, Yu C. Experiments and simulations of cold-formed steel wall assemblies using corrugated steel sheathing subjected to shear and gravity loads. ASCE J Struct Eng 2017;143(3):04016193.
- [19] Fülöp A, Dubina D. Performance of wall-stud cold-formed shear panels under monotonic and cyclic loading. Part I: experimental research. Thin-Walled Struct 2004;42(2):321–38.
- [20] Sharafi P, Mortazavi M, Usefi N, Kildashti K, Ronagh H, Samali B. Lateral force

- resisting systems in lightweight steel frames: recent research advances. *Thin-Walled Struct* 2018;130:231–53.
- [21] Rizk R. Cold-formed steel frame - steel sheathed shear walls: improved range of shear strength values accounting for effect of full frame blocking and thick sheathing/framing members. Master's thesis. Montreal, Canada: Department of Civil Engineering and Applied Mechanics, McGill University; 2017.
- [22] Brière V. Higher capacity cold-formed steel sheathed and framed shear walls for mid-rise buildings: Part 2. Master's thesis. Montreal, Canada: Department of Civil Engineering and Applied Mechanics, McGill University; 2017.
- [23] Santos V. Higher capacity cold-formed steel sheathed and framed shear walls for mid-rise buildings: Part 1. Master's thesis. Montreal, Canada: Department of Civil Engineering and Applied Mechanics, McGill University; 2017.
- [24] Yanagi N, Yu C. Effective strip method for the design of cold-formed steel framed shear wall with steel sheet sheathing. *ASCE J Struct Eng* 2014;140(4):1–8.
- [25] American Iron and Steel Institute (AISI). North American specification for the design of cold-formed steel structural members. AISI S100-16, Washington, USA; 2016.
- [26] Canadian Standards Association (CSA). North American specification for the design of cold-formed steel structural members. CSA S136-16, Rexdale, Canada; 2016.
- [27] Krawinkler H, Parisi F, Ibarra L, Ayoub A, Medina R. Development of a testing protocol for woodframe structures. Report W-02 covering Task 1.3.2, CUREE/Caltech Woodframe Project. Richmond, USA: Consortium of Universities for Research in Earthquake Engineering (CUREE); 2000.
- [28] American Society for Testing and Materials (ASTM). Standard test methods for cyclic (reversed) load test for shear resistance of vertical elements of the lateral force resisting systems for buildings. ASTM E2126. West Conshohocken, USA; 2011.
- [29] Park R. Evaluation of ductility of structures and structural assemblages from laboratory testing. *Bull NZ Natl Soc Earthq Eng* 1989;22(3):155–66.
- [30] Foliente GC. Issues in seismic performance testing and evaluation of timber structural systems. In: Proceedings international wood engineering conference. New Orleans, USA, 1, 29–36; 1996.
- [31] Branston AE, Boudreault FA, Chen CY, Rogers CA. Testing of light-gauge steel frame – wood structural panel shear walls. *Can J Civil Eng* 2006;33(7):561–72.
- [32] Branston AE, Boudreault FA, Chen CY, Rogers CA. Light-gauge steel-frame – wood structural panel shear wall design method. *Can J Civil Eng* 2006;33(7):872–89.
- [33] National Research Council of Canada (NRC). National building code of Canada. 13th ed. Ottawa, Canada; 2015.
- [34] American Society of Civil Engineers (ASCE). Minimum design loads for buildings and other structures. ASCE/SEI 7-16. Reston, USA; 2016.